International Journal of Engineering

Multi-Dimensional Modeling of the Effects of Spilt Injection Scheme on Performance and Emissions of IDI Diesel Engines

S. Jafarmadar*, A. Zehni

Department of mechanical Engineering, University of Urmia, Urmia, Iran

A R T I C L E   I N F O

A B S T R A C T

One of the important problems in reducing of pollutant emission from DI and IDI diesel engines is trade-off between soot and NOx. Split injection is one of the most powerful tools that makes the chance to shift the trade-off curve closer to origin. At the present work, the effect of split injection on the combustion process and emissions of a cylinder IDI diesel engine under the specifications of 5.9 kW maximum engine power and engine speed of 730 rpm has been investigated. The studies of injection timing and split injection parameters, including the delay dwell and the fuel quantity injected between injection pulses are carried out. Three different split injection schemes, in which 10, 20 and 25% of total fuel injected in the second pulse, have been considered. The numerical results show that 25% of total fuel injected in the second pulse which is accompanied with the 20ºCA delay dwell between injections, reduces the total soot and NOx emissions effectively in IDI diesel engines. The predicted values of combustion process and emissions by the model at baseline engine show a good agreement with the corresponding experimental data. This agreement makes the model a reliable tool that can use for exploring new engine concepts.

1. INTRODUCTION[1]

The major pollutants from diesel engines are NOx and soot. NOx and soot emissions are of concerns to the international community. They have been judged to pose a lung cancer hazard for humans as well as elevating the risk of non-cancer respiratory ailments. These emissions react in the atmosphere in the presence of sunlight to form ground-level ozone. Ground-level ozone is a major component of smog in our cities and in many rural areas as well. In addition, NOx reacts with water, oxygen and oxidants in the atmosphere to form acid rain. Furthermore, the indirect effect of NOx emissions to global warming should be noted.

Stringent exhaust emission standards require the simultaneous reduction of soot and NOx for diesel engines. However it seems to be very difficult to reduce NOx emission without increasing soot emission. The reason is that always there is a contradiction between NOx and soot emissions whenever the injection timing is retarded or advanced.

Split injection has been shown to be a powerful tool to simultaneously reduce soot and NOx emissions for DI and IDI diesel engines when the injection timing is

optimized. It is defined as splitting the main single injection profile in two or more injection pulses with definite delay dwell between the injections. However, an optimum injection scheme of split injection for DI and IDI diesel engines has been always under investigation.

Generally, the exhaust of IDI diesel engines are less smoky when compared to DI diesel engines [1]. Hence, investigation the effect of split injection on combustion process and pollution reduction of IDI diesel engines can be quite valuable.

In an IDI diesel engine, the combustion chamber is divided into the pre-chamber and the main chamber, which are linked by a throat. Fuel injects into the pre-combustion chamber and air is pushed through the narrow passage on the compression stroke and becomes turbulent within the pre-chamber. This narrow passage speeds up the expanding gases more. The pre-chamber approximately contains 50% of the combustion volume when the piston is at TDC. This geometrical represents an additional difficulty to those deals with in the DI combustion chambers.

In the recent years, the main recent studies about the effect of the split injection on the combustion process and pollution of DI and IDI diesel engines are as follows:

*Corresponding author: Email- S.Jafarmadar@Urmia.ac.ir

Bianchi et al [2] investigated the capability of split injection in reducing NOx and soot emissions of HSDI Diesel engines by CFD code KIVA-III. Computational results indicate that split injection is very effective in reducing NOx, while soot reduction is related to a better use of the oxygen available in the combustion chamber.

Tatschi et al [3] studied the impact of combustion variations such as EGR (exhaust gas recirculation), SOI (start of injection) and split injection in a turbo-charged DI diesel engine by the CFD code FIRE. The predicted values by the modeling, showed a good agreement with the experimental data.

Shayler and Ng [4] used the KIVA-III to investigate the influence of split main ratio and delay dwell on NOx and soot emissions. Numerical conclusions showed that when delay dwell is small, soot is lowered but NOx is increased. In addition, when delay dwell is large, the second injection has very little influence on soot production and oxidation associated with the first injection.

Chryssakis et al [5] studied the effect of multiple injections on combustion process and emissions of a DI diesel engine using the multidimensional code KIVAIII. The results indicated that employing a post-injection combined with a pilot injection results in reduced soot formation; while the NOx concentration is maintained in low levels.

Lechner et al [6] analyzed the effect of spray cone angle and advanced injection-timing strategy to achieve partially premixed compression ignition (PCI) in a DI diesel engine. The authors proved that low flow rate of the fuel; 60-degree spray cone angle injector strategy, optimized EGR and split injection strategy could reduce the engine NOx emission by 82% and particular matter by 39%.

Ehleskog [7] investigated the effect of split injection on the emission formation and engine performance of a heavy-duty DI diesel engine by KIVA-III code. The results revealed that reductions in NOx emissions and brake-specific fuel consumption were achieved for short dwell times whereas they both were increased when the dwell time was prolonged.

Sun and Reitz [8] studied the combustion and emission of a heavy-duty DI diesel engine by multi-dimensional Computational Fluid Dynamics (CFD) code with detailed chemistry, the KIVA-CHEMKIN. The results showed that the start of late injection timing in two-stage combustion in combination with late IVC timing and medium EGR level was able to achieve low engine-out emissions.

Verbiezen et al [9] investigated the effect of injection timing and split injection on NOx concentration in a DI diesel engine experimentally. The results show that advance of the injection timing causes an increase in NOx. Also, maximum rate of heat release is significantly reduced by the split injection. Hence, NOx is reduced significantly.

Abdullah et al [10] progressed an experimental research for optimizing the variation of multiple injections on the engine performance and emissions of a DI diesel engine. The results depict that, the combination of high pressure multiple injections with cooled EGR produces better overall results than the combination of low injection pressure multiple injections without EGR.

Jafarmadar and Zehni [11] studied the effect of split injection on combustion and pollution of a DI diesel engine by Computational Fluid Dynamics (CFD) code. The results also show that 25% of total fuel injected in the second pulse, reduces the total soot and NOx emissions effectively in DI diesel engines. In addition, the optimum delay dwell between the two injection pulses was about 25ºCA.

Showry and Rajo [12] carried out the effect of triple injection on combustion and pollution of a DI diesel engine by FLUENT CFD code and concluded that 10° is an optimum delay between the injection pulses for triple injection strategy.

As mentioned, the effect of split injection on combustion and emission of DI Diesel engines has been widely studied up to now. However, for IDI diesel engines, the study of split injection strategy in order to reduce emissions is confined to the research of Iwazaki et al [13] that investigated the effects of early stage injection and two-stage injection on the combustion characteristics of an IDI diesel engine experimentally. The results indicated that NOx and smoke emissions were improved by two-stage injection when the amount of fuel in the first injection was small and the first injection timing was advanced from -80 to -100° TDC.

The present work is the continued study of the reference [11]. It means that the effect of the split injection on combustion and pollution of IDI diesel engines is studied at full load state by the CFD code. The target is to obtain the optimum split injection case in which the total exhaust NOx and soot concentrations are more reduced than the other cases. Three different split injection schemes, in which 10, 20 and 25% of total fuel injected in the second pulse, have been considered. The delay dwell between injections is varied from 5°CA to 30°CA with the interval 5°CA.

2. MATERIALS AND METHODS

2.1. Initial and Boundary Conditions   Calculations are carried out on the closed system from Intake Valve Closure (IVC) at 165°CA BTDC to Exhaust Valve Open (EVO) at 180°CA ATDC. Fig. 1-a and Fig. 1-b show the numerical grid, which is designed to model the geometry of combustion chamber and contains a maximum of 42200 cells at BTDC. As can be seen from Fig. 1-c, Grid dependency is based on the in-cylinder pressure and present resolution is found to give adequately grid independent results. There is a single hole injector mounted, which is in pre-chamber as

shown in Fig. 2. Initial pressure in the combustion chamber is set to 86 kPa and initial temperature is calculated to be 384K, and swirl ratio is assumed to be on quiescent condition. Boundary temperatures in the combustion chamber are as follow:
Head temperature: 550K.
Piston temperature: 590K.
Cylinder temperature: 450K.
Present work is studied at full load mode and the engine speed is 730 rev/min. All boundary temperatures were assumed to be constant throughout the simulation, but allowed to vary with the combustion chamber surface regions.
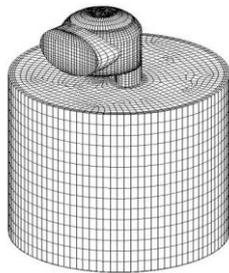

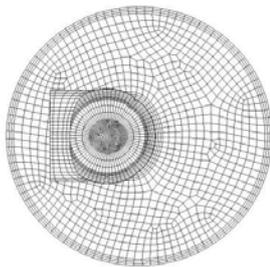**Fig. 1-a.** Mesh of the Lister 8.1 indirect injection diesel engine.
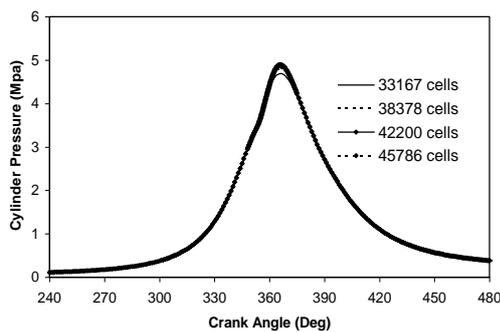

Fig. 1-b. Top view of the mesh.

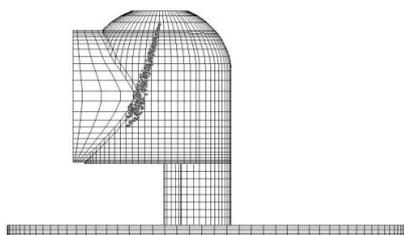**Fig. 1-c.** Grid dependency based on the in-cylinder pressure

Fig. 2. Spray and injector coordinate at pre-chamber

2.2. Model Formulation   The numerical model is carried out for Lister 8.1 indirect injection diesel engine with the specification on Table 1. The governing equations for unsteady, compressible, turbulent reacting multi-component gas mixtures flow and thermal fields are solved from IVC to EVO by the commercial AVL-FIRE CFD code [14]. The turbulent flow within the combustion chamber is simulated using the RNG k-ε turbulence model, modified for variable-density engine flows [15].

The standard WAVE model, described in [16], is used for the primary and secondary atomization modeling of the resulting droplets. At this model, the growth of an initial perturbation on a liquid surface is linked to its wavelength and other physical and dynamical parameters of the injected fuel at the flow domain. Drop parcels are injected with characteristic size equal to the Nozzle exit diameter (blob injection).

TABLE 1. Specifications of Lister 8.1 IDI diesel engine

Cycle Type	Four Stroke
Number of Cylinders	1
Injection Type	IDI
Cylinder Bore	114.1 mm
Stroke	139.7 mm
L/R	4
Displacement Volume	1.43 lit.
Compression Ratio	17.5 : 1
Vpre-chamber/VTDC	0.7
Full Load Injected Mass	$6.4336e-5$ kg per Cycle
Power on 850 rpm	5.9 kW
Power on 650 rpm	4.4 kW
Initial Injection Pressure	90 bar
Nozzle Diameter at Hole Center	0.003m
Number of Nuzzle Holes	1
Nozzle Outer diameter	0.0003m
Spray Cone Angle	10°
Valve Timing	IVO= 5° BTDC
	IVC= 15° ABDC
	EVO= 55° BBDC
	EVC= 15° ATDC

The Dukowicz model is applied for treating the heat up and evaporation of the droplets, which is described in [17]. This model assumes a uniform droplet temperature. In addition, the droplet temperature change rate is determined by the heat balance, which states that the heat convection from the gas to the droplet either heats up the droplet or supplies heat for vaporization.
A Stochastic dispersion model was employed to take the effect of interaction between the particles and the turbulent eddies into account by adding a fluctuating velocity to the mean gas velocity. This model assumes that the fluctuating velocity has a randomly Gaussian distribution [14].
The spray/wall interaction model used in this simulation was based on the spray/wall impingement model [18]. This model assumes that a droplet, which hits the wall is affected by rebound or reflection based on the Weber number.

The Shell auto-ignition model was used for modeling of the auto ignition [19]. In this generic mechanism, six generic species for hydrocarbon fuel, oxidizer, total radical pool, branching agent, intermediate species and products were involved. In addition, the important stages of auto ignition such as initiation, propagation, branching and termination were presented by generalized reactions, described in [14, 19].

The Eddy Break-up model (EBU) based on the turbulent mixing is used for modeling of the combustion in the combustion chamber [14]. This model assumes that in premixed turbulent flames, the reactants (fuel and oxygen) are contained in the same eddies and are separated from eddies containing hot combustion products. The rate of dissipation of these eddies determines the rate of combustion. In other words, chemical reaction occurs fast and the combustion is mixing controlled. NOx formation is modeled by the Zeldovich mechanism and Soot formation is modeled by Kennedy, Hiroyasu and Magnussen mechanism [20].

The injection rate profile is rectangular type and consists of nineteen injection schemes, i.e. single injection and eighteen split injection cases. To simulate the split injection, the original single injection profile is divided into two injection pulses without altering the injection profile and magnitude. Fig. 3 illustrates the schematic scheme of the single and split injection strategy.
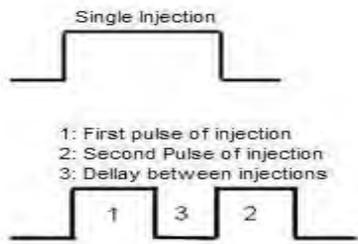

Fig. 3. schematic scheme of single and split injection strategy.

For the single injection case, the start of injection is at 348°CA and injection termination is at 387°CA. For all split injection cases, the injection timing of the first injection pulse is fixed at 348°CA. Three different split injection schemes, in which 10-20-25% of total fuel injected in the second pulse, has been considered. The delay dwell between injections is varied from 5°CA to 30°CA with the interval 5°CA.

2.3. Performance Parameters   Indicated work per cycle was calculated from the cylinder pressure and piston displacement, as follows:

$$W = \int_{\theta_1}^{\theta_2} P dV \qquad (1)$$

where, θ_1, θ_2 are the start and end of the valve-closed

period, respectively (i.e. IVC= 15° ABDC and EVO= 55° BBDC). The indicated power per cylinder and indicated mean effective pressure were related to the indicated work per cycle by:

$$P(kW) = \frac{W(N.m)N(rpm)}{60000n} \qquad (2)$$

$$IMEP = \frac{W}{V_d} \qquad (3)$$

where, n=2 is the number of crank revolutions for each power stroke per cylinder, N is the engine speed rpm and V_d is volume displacement of piston. The brake specific fuel consumption (BSFC) was defined as:

$$BSFC = \frac{\dot{m}_f}{p_b} \qquad (4)$$

In Equation (1), the work was only integrated as part of the compression and expansion strokes; the pumping work has not been taken into account. Therefore, the power and ISFC analyses can only be viewed as being qualitative rather than quantitative in this study.

3. RESULTS AND DISCUSSION

Figs. 4 and 5 show the verification of computed and measured [21] mean in-cylinder pressure and heat release rate for the single injection case. They show that both computational and experimental data for cylinder pressure and heat release rate during the compression and expansion strokes are in good agreement.

The peak of cylinder Pressure is 4.88 Mpa, which occurs at 366°CA (4°CA after TDC). The start of heat release is at 351°CA for computed and measured results; in other words, the ignition delay dwell is 3°CA. It means that the ignition delay is quite close to the chemical ignition delay and that the physical ignition delay is very short, because of the rapid evaporation of the small droplets injected through the small injector gap at the start of injection. The heat release rate, which called "measured", is actually derived from the procured in-cylinder pressure data using a thermodynamic first law analysis as followed:

$$\frac{dq}{d\theta} = \frac{\gamma}{\gamma - 1} p \frac{dV}{d\theta} + \frac{1}{\gamma - 1} V \frac{dp}{d\theta} \qquad (5)$$

where P and V are in-cylinder pressure and volume versus the crank angle θ, and γ=1.33.

The main difference of computed and measured HRR is due to the premixed combustion. The peak of computed HRR is 59J/deg that occurs at 364°CA, compared to the peak of measured HRR that is 53J/deg at 369°CA.

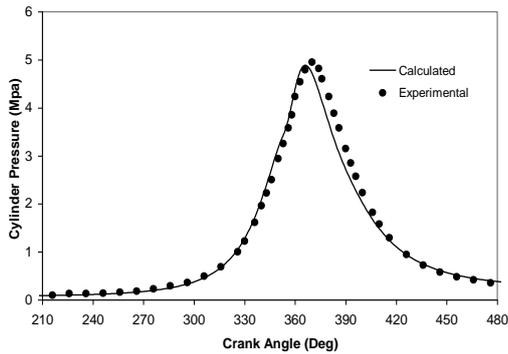As a whole, the premixed combustion occurs with a steep slope and it can be one of the major sources of NOx formation.

Fig. 4. comparison of calculated and measured [21] in-cylinder pressure, single injection case
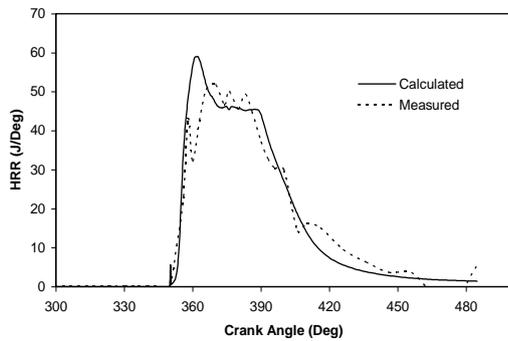

Fig. 5. comparison of calculated and measured [21] heat release rate, single injection case

Table 2 shows the variation of performance parameters for the single injection case, compared with the experimental data [21]. In contrast with the experimental results, it can be seen that model can predict the performance parameters with good accuracy.

TABLE 2. Comparison of calculated and measured [21] performance parameters, single injection case

	Calculated	Experimental
Indicate Power [kW]	5.34	-----------------
Brake Power [kW]	4.53	4.65
$\dot{m}_{fuel}$ [g/sec]	0.391	0.391
BMEP [Bar]	5.33	5.47
BSFC [g/kW.h]	310.72	302.7

Fig. 6 indicates that the predicted total in-cylinder NOx emission for the single injection case, agrees well with the engine-out measurements [21]. Heywood [22] explains that the critical time for the formation of oxides of nitrogen in compression ignition engines is between the start of combustion and the occurrence of peak cylinder pressure when the burned gas temperatures are the highest. The trend of calculated NOx formation in the pre-chamber and main chambers agrees well with the Heywood's explanations. As temperature cools due

to volume expansion and mixing of hot gases with cooler burned gas, the equilibrium reactions are quenched in the swirl chamber and main chamber. As can be seen from the fig. 7, the predicted total in-cylinder soot emission for the single injection case, as well as calculated NOx, agrees well with the engine-out measurements [21].
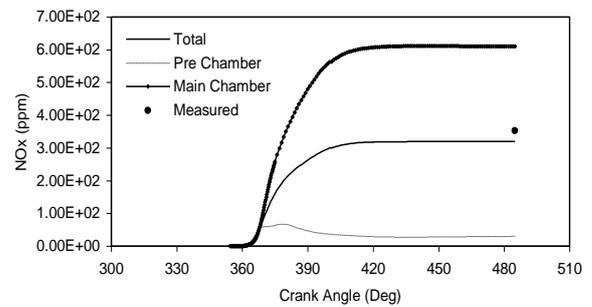

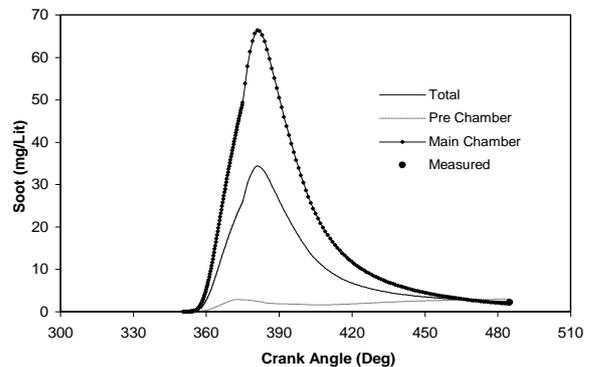**Fig. 6.** comparison of calculated and measured [21] NOx emission, single injection case

Fig. 7. comparison of calculated and measured [21] Soot emission, single injection case

Table 3 presents the exhaust NOx and soot emissions and performance parameters for the calculated single injection, and split injection cases. As can be seen, the lowest NOx and Soot emissions are related to the 75%-15-25% and 75%-20-25% cases respectively. In order to obtain the final optimum case, i.e. the case that involves the highest average of NOx and Soot reduction, a new dimensionless parameter is defined as:
The more of the total   average emission reduction percentage results to the better optimum split injection case. Hence, it is concluded that the 75%-20-25% scheme with the average reduction percentage of 23.28 is the optimum injection case.
In addition, it can be deduced from the Table 3 that in general, split injection sacrifices the brake power and Bsfc of the engine. This result is more apparent for the 80%-20% and 75%-25% cases. The reason is that with reduction of the first pulse of injection and increase of delay dwell between injections, premixed combustion as the main source of the power stroke is decreased.

TABLE 3. Exhaust emissions and performance parameters for the single injection and split injection cases

	NOx (ppm)	Soot (mg/lit)	NOx Reduction (%)	Soot Reduction (%)	Average reduction (%)	Pb (kW)	Bsfc (gr/kw.h)
Single Inj	320	2.4	0	0	0	4.53	310.72
90%-5-10%	316	1.9	1.25	20.83	11.04	4.51	312.1
90%-10-10%	309	1.75	3.43	27.08	15.25	4.4	319.9
90%-15-10%	300	1.62	6.25	32.5	19.37	4.32	325.8
90%-20-10%	311	1.72	2.81	28.33	15.57	4.37	322.1
90%-25-10%	303	1.69	5.31	29.58	17.44	4.33	325.08
90%-30-10%	305	1.7	4.68	29.16	16.92	4.35	323.58
80%-5-20%	318	1.99	0.6	17.08	8.84	4.36	322.84
80%-10-20%	303	1.81	5.31	24.58	14.94	4.31	326.58
80%-15-20%	303	1.74	5.31	27.5	16.4	4.2	335.14
80%-20-20%	302	1.64	5.62	31.66	18.64	4.14	340
80%-25-20%	303	1.62	5.31	32.5	18.9	4.13	340.82
80%-30-20%	300	1.59	6.25	33.75	20	4.12	341.65
75%-5-25%	306	2	4.37	20	12.18	4.29	328.11
75%-10-25%	305	1.93	4.68	19.58	12.13	4.18	336.74
75%-15-25%	*298*	1.58	6.87	34.16	20.51	4.12	341.65
75%-20-25%	299	*1.44*	6.56	40	*23.28*	4.04	348.41
75%-25-25%	302	1.52	5.62	36.66	21.14	4	351.9
75%-30-25%	299	1.56	6.56	35	20.78	3.97	354.55

Hence, Bsfc is increased as well. As can be seen, the lowest brake power and highest Bsfc are related to the 75%-30-25% case.

Fig. 8 shows the NOx versus Soot emission for the single injection and split injection cases. As can be seen, the 75%-20-25% case is closer to origin, i. e. zero emission. Hence, this confirms that the case of 75%-20-25% is the optimum case.
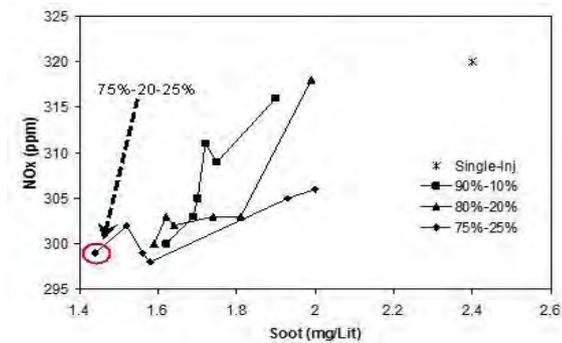
Fig. 8. NOx versus soot emission for the single injection and split injection cases

It is of interest to notify that the optimum injection scheme for DI diesel engine at full load state is 75%-25-25% [11]. It means that the first and second injection pulses for the DI and IDI diesel engines are the same. The difference is related to the delay dwell between injections. I.e. the delay dwell for the optimum IDI split injection case because of high turbulence intensity an fast combustion is 5°CA lower than the optimum DI split injection case.

It is noticeable to compare the spray penetration, in-cylinder flow field, combustion and emission characteristics of the single injection and optimum injection cases to obtain valuable results.

The normalized injection profile versus crank angle for the single injection and 75%-20-25% cases is shown in the Fig. 9.
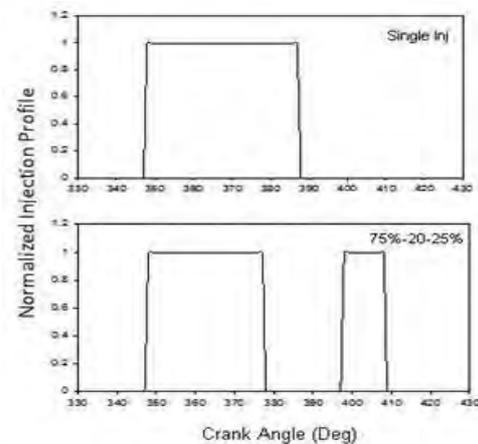

Fig. 9. The normalized injection profile versus crank angle for the single injection and 75%-20-25% cases

Fig. 10-a and Fig. 10-b represent respectively front and top views of the evolution of the spray penetration and velocity field at various crank angles in horizontal planes of the pre and main combustion chambers and planes across the connecting throat for the single injection and 75%-20-25% cases. It can be seen that the maximum velocity at whole crank angles because of the large area at throat section are lower than the other data in the literatures [23]. Generally, for all the cases, the maximum velocity of the flow field is observed at the tip of the spray, swirl chamber throat and some areas of the main chamber that is far from the cylinder wall and cylinder head.
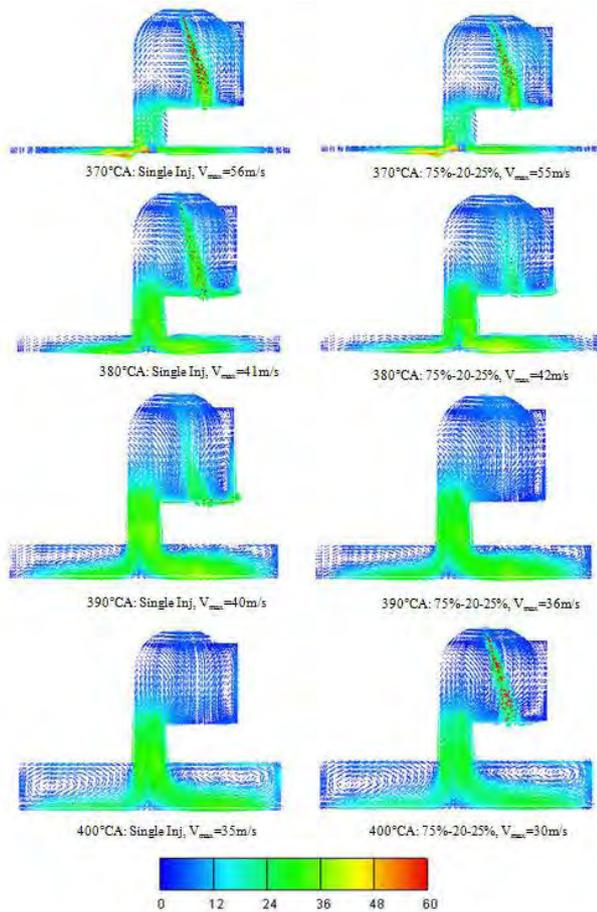
Fig. 10-a. Comparison of spray penetration and velocity filed at various crank angles for the single injection and 75%-20-25% cases, front view.

Fig. 10-b. Comparison of spray penetration and velocity filed at various crank angles for the single injection and 75%-20-25% cases, top view.

As can be seen, at various crank angles, the main difference of the in-cylinder flow field between the single injection and split injection cases is due to the fuel injection scheme. In other words, the amount of the fuel spray and the crank position in which the spray is injected. The aerodynamic forces decelerate the droplets for the both cases. The drops at the spray tip face the strongest drag force and are much more decelerated than droplets that follow in their wake.

At 370°CA, air entrainment into the fuel spray can be observed for the both cases. Hence, Droplet velocities are maximal at the spray axis and decrease in the radial direction due to interaction with the entrained gas.

Although the amount of the fuel spray for the single injection case is higher than the 75%-20-25% case at 370°CA, the flow field difference is not observed obviously. The more quantity of the fuel spray for the single injection case causes the maximum velocity of the single injection case to be higher about 1m/s than
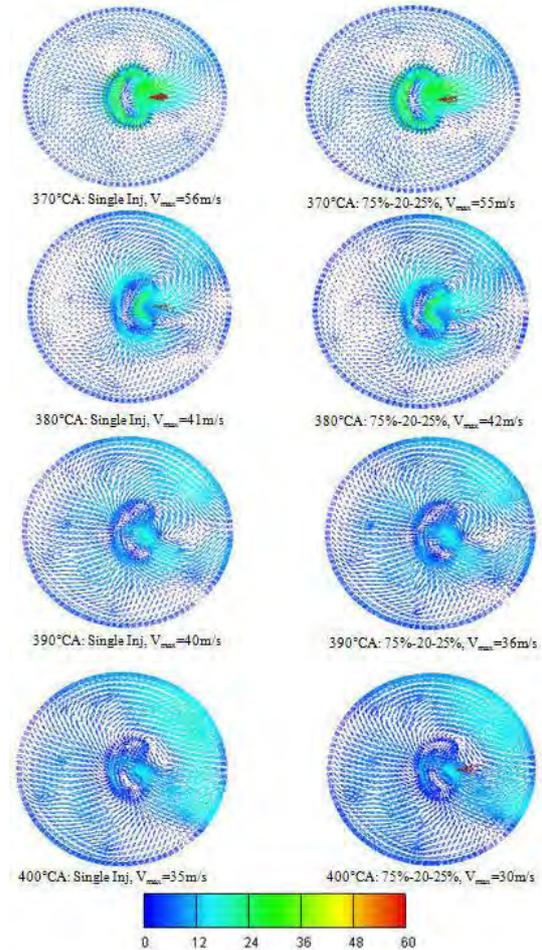
the 75%-20-25% case.

At 380°CA, the fuel spray is cut off for the 75%-20-25% case. Since the entrained gas into to the spray region is reduced, the flow moves more freely from the swirl chamber to the main chamber. Hence, as can be seen from the front view, the maximum flow field velocity for the 75%-20-25% case is higher compared to the single injection case.

At 390°CA, from the top view, the distribution of the flow field in the whole of the main chamber is visible. In addition, some local swirls can be seen in the main chamber that are close to the swirl chamber. From the front view, it is observed that the gas coming from the pre-chamber reaches the opposite sides of cylinder wall.This leads to the formation of the two eddies occupying each one-half of the main chamber and staying centered with respect to the two half of the bowl.

The start of the second injection pulse for the 75%-

20-25% case is perceived At 400°CA. since the swirl intensity in the swirl chamber is reduced at this crank position, the interaction between the flow field and spray is decreased to somehow. Flow in the pre-chamber is not also strongly influenced by the fuel spray. Hence, the maximum velocity of the flow field for the 75%-20-25% case remains lower compared to the single injection case.

Fig. 11 indicates the history of heat release rate, cylinder pressure, temperature, O_2 mass fraction, NOx and soot emissions for the single injection and 75%-20-25% cases.
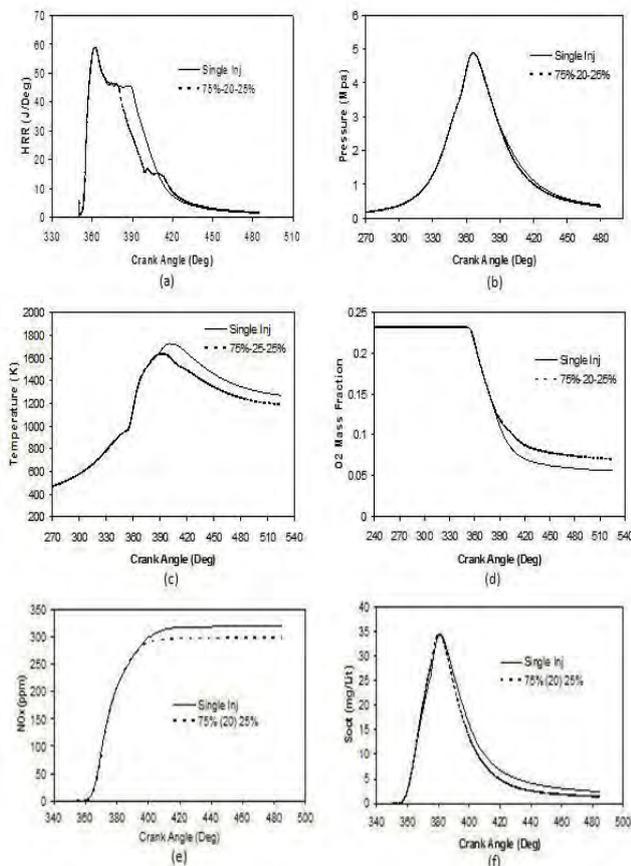

Fig. 11. Comparison of HRR, cylinder pressure and temperature, O_2 mass fraction, NOx and soot histories for the single injection and 75%-20-25% cases.

Fig. 11-a shows that the amount of heat release rate for the both cases is to somehow equal until 380°CA. It is due to the fact that the first injection pulse for the 75%-20-25% case, lasts to 377°CA. Hence, the premixed combustion for the both cases does not differ visibly. For the 75%-20-25% case, The second peak of heat release rate occurs at 410°CA and indicates that a rapid diffusion burn is realized at the late combustion stage and it affects the in-cylinder pressure, temperature and soot oxidation.

Fig. 11-b shows that the second injection pulse of

the 75%-20-25% does not cause to the second peak of the cylinder pressure. It is because the rate of decrease of cylinder pressure due to the expansion stroke is almost equal to the rate of increase of cylinder pressure due to the diffusion combustion.

Fig. 11-c compares temperature trend for 75%-20-25% and single injection cases. As can be seen, for the 75%-20-25% case, the peak of the temperature advances about 11°CA compared to the peak of the temperature of the single injection case. In addition, the temperature reduction reaches to 90°K.

Fig. 11-d presents the in cylinder O2 mass fraction. It can be seen that after 385°CA, the O2 concentration for the 75%-20-25% case is higher than that for the single injection case. In other words, oxygen availability of 75%-20-25% case is better.

As Fig. 11-e and Fig. 11-f indicate, the reduction of the peak of the cylinder temperature for the 75%-20-25% case, causes to the lower NOx formation. In addition, soot oxidation for the 75%-20-25% case is higher compared to that for the single injection case. It is because for the 75%-20-25% case, the more availability of oxygen in the expansion stroke compensates the decrease of temperature due to the split injection. Hence, soot oxidation is increased.

Fig. 12-a and Fig. 12-b represent respectively front and top views of the contours of equivalence ratio, temperature, NOx and soot emissions at various crank angles in horizontal planes of the main combustion chamber and planes across the connecting throat for the single injection and 75%-20-25% cases.

At 400°CA, for the both cases, the majority of NOx is located in the two half of the main chamber, whilst soot is concentrated in the swirl chamber, throat section and main chamber. For the both cases, a local soot-NOx trade-off is evident in the swirl chamber, as the NOx and soot formation occur on opposite sides of the high temperature region. Equivalence ratio contour of the 75%-20-25% case confirms that injection termination and resumption, causes leaner combustion zones. Hence, the more reduction of soot for the 75%-20-25% is visible compared to the single injection case.

NOx and soot formation depend strongly on equivalence ratio and temperature. It is of interest to notice that the area which the equivalence ratio is close to 1 and the temperature is higher than 2000 K is the NOx formation area. In addition, the area which the equivalence ratio is higher than 3 and the temperature is approximately between 1600 K and 2000 K is the Soot formation area. The area from 1500 K and equivalence ratio near to 1 is defined as soot oxidation area [24, 25]. At 410°CA, due to the second injection pulse, increase of the equivalence ratio is observed in the swirl chamber of the 75%-20-25% case. Hence, the enhancement of the soot concentration close to the wall spray impingement is observed. For the other areas, soot oxidation for the 75%-20-25% case is higher compared
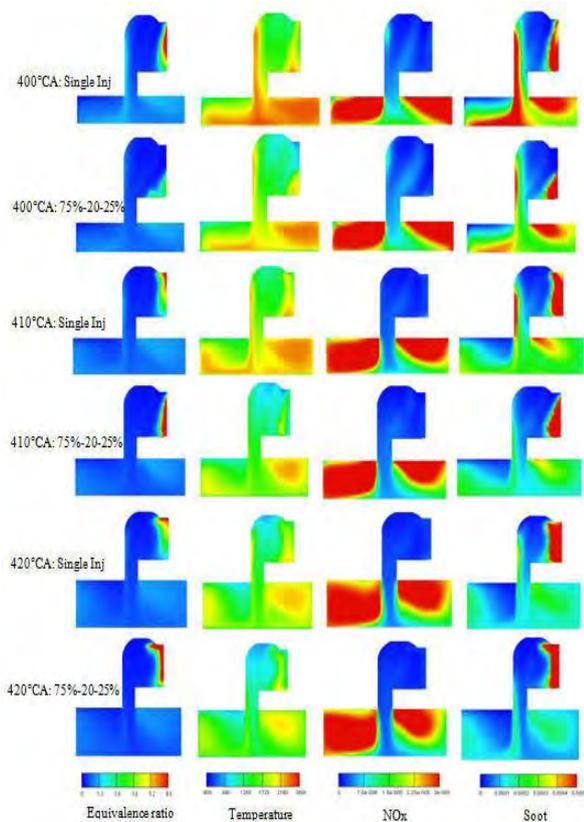
Fig. 12-a. Contours of equivalence ratio, Temperature, NOx and Soot at different crank angles, front view

Fig. 12-b. Contours of equivalence ratio, Temperature, NOx and Soot at different crank angles, top view.

to the single injection case. In addition, NOx reduction tendency is visible in the right side of the main chamber of the 75%-20-25% case compared to the single injection case. It is because more temperature reduction occurs for the 75%-20-25% case due to the lower premixed combustion. The diffusion combustion of the second injection pulse does not affect NOx formation significantly.

The final form of the distribution of equivalence ratio, temperature, NOx and soot contours can be seen at 420°CA. The reduction of soot and NOx for the 75%-20-25% case is clear compared to the single injection case. This trend is preserved for the both cases until EVO.

4. CONCLUSION

At the present work, the effect of the split injection on combustion and pollution of IDI diesel engines was studied at full load state by the CFD code. The target was to obtain the optimum split injection case in which the total exhaust NOx and soot concentrations were the lowest.

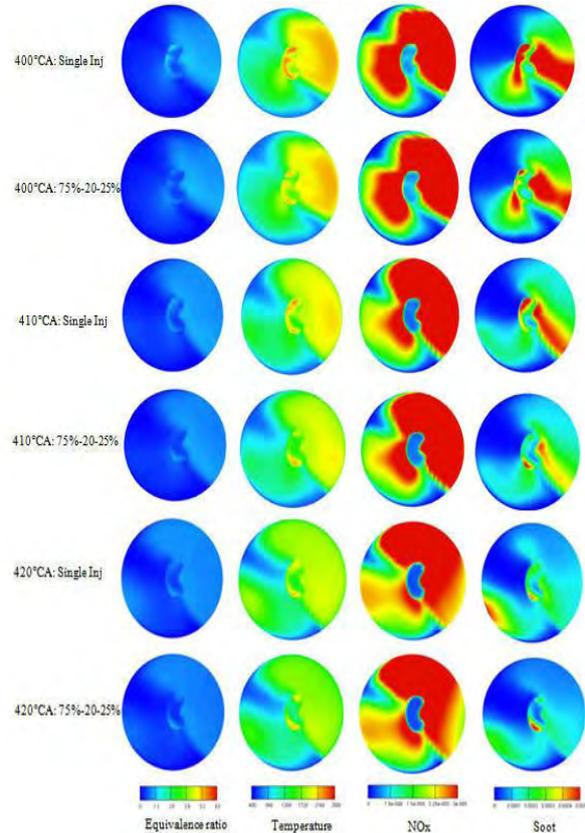Three different split injection schemes, in which 10,

20 and 25% of total fuel injected in the second pulse, was considered. The delay dwell between injections pulses was varied from 5°CA to 30°CA with the interval 5°CA.The results are as follows:

1. The calculated combustion and performance parameters, exhaust NOx and soot emissions for the single injection case showed a good agreement with the corresponding experimental data.

2. The lowest NOx and Soot emissions are related to the 75%-15-25% and 75%-20-25% cases respectively. Finally, optimum case was 75%-20-25% regarding the highest average of NOx and soot reduction.

3. The lowest brake power and highest Bsfc quantity is due to the 75%-30-25% case.

4. Since in the literature, the optimum split injection scheme for DI diesel engines at full state was defined as 75%-25-25%, it was concluded that the difference of the optimum split injection scheme for DI and IDI diesel engines was related to the delay dwell between the injections.

5. The main difference of the in-cylinder flow field between the single injection and split injection cases is due to the fuel injection scheme.

6. For the 75%-20-25% case, the more availability of oxygen in the expansion stroke compensates the

decrease of temperature due to the split injection. Hence, soot oxidation is increased.

7. The final form of the NOx and soot at 420°CA which preserve it's trend until EVO, confirms the more reduction of NOx and soot for the 75%-20-25% case in comparison with the single injection case.

5. REFERENCES

1. Gomaa, M., Alimin, A. J. and Kamarudin, K. A., "Trade-off between NOx, soot and EGR rates for an IDI diesel engine fuelled with JB5", *World Academy of Science, Engineering and Technology*, Vol. 62, (2010), 449-450.

2. Bianchi, G. M., Peloni, P., Corcione, F. E. and Lupino, F., "Numerical analysis of passenger car HSDI diesel engines with the 2nd generation of common rail injection systems: The effect of multiple injections on emissions", SAE Paper NO. 2001-01-1068; 2001.

3. Tatschi, R., Gabrief, H. P. and Priesching, P., "Fire-a generic CFD platform for DI diesel engine mixture formation and combustion simulation", User's group meeting at the SAE congress march 4; 2001.

4. Shayler, P. j. and Ng, H. K., "Simulation studies of the effect of fuel injection pattern on NOx and soot formation in diesel engines", SAE Paper NO. 2004-01-0116; 2004.

5. Chryssakis, C. A., Assanis, D. N., Kook, S. and Bae, C., "Effect of multiple injections on fuel-air mixing and soot formation in diesel combustion using direct flame visualization and CFD techniques", Spring Technical Conference, ASME NO. ICES2005-1016; 2005.

6. Lechner, G. A., Jacobs, T. J., Chryssakis, C. A., Assanis, D. N. and Siewert, R. M., "Evaluation of a narrow spray cone angle, advanced injection strategy to achieve partially premixed compression ignition combustion in a diesel engine, "SAE Paper No. 2005-01-0167; 2005.

7. Ehleskog, R., "Experimental and numerical investigation of split injections at low load in an HDDI diesel engine equipped with a piezo injector", SAE Paper NO. 2006-01-3433; 2006.

8. Sun, Y. D. and Reitz, R., "Modeling diesel engine NOx and soot reduction with optimized two-stage combustion", SAE Paper No. 2006-01-0027; 2006.

9. Verbiezen, K., Donkerbroek, A. J., Klein-Douwel, R. J. H., Vliet, A. P. van., Frijters, P. J. M., Seykens, X. L. J., Baert, R. S. G., Meerts, . W. L., Dam, N. J. and Meulen, J. J., "Diesel combustion: in-cylinder NO concentrations in relation to injection timing", *Combustion and Flame*, Vol. 151, (2007), 333–346.

10. Abdullah, N., Tsolakis, A., Rounce, P., Wyszinsky, M., Xu, H. and Mamat, R., "Effect of injection pressure with split injection in a V6 diesel engine", SAE Paper NO. 2009-24-0049; 2009.

11. Jafarmadar, S. and Zehni, A., "Multi-dimensional modeling of the effects of split injection scheme on combustion and emissions of direct-injection diesel engines at full load state", *Iranian Journal of Engineering*, Vol. 22, No. 4, (2009).

12. Showry, K. and Raju, A., "Multi-dimensional modeling and simulation of diesel engine combustion using multi-pulse injections by CFD", *International Journal of Dynamics of Fluids*, Vol. 6, No. 2, (2010), 237–248.

13. Iwazaki, K., Amagai, K. and Arai, M., "Improvement of fuel economy of an indirect (IDI) diesel engine with two-stage injection", *Energy Conversion and Management*, Vol. 30, (2005), 447-459.

14. AVL FIRE user manual V. 8.5, 2006.

15. Han, Z. and Reitz, R. D., "Turbulence modeling of internal combustion engines using RNG K-ε models", *Combustion Science and Technology*, Vol. 106, No. 4, (1995), 267-295.

16. Liu, A. B. and Reitz, R. D., "Modeling the effects of drop drag and break-up on fuel sprays", SAE Paper NO. 930072; 1993.

17. Dukowicz, J. K., "Quasi-steady droplet change in the presence of convection", Informal report Los Alamos Scientific Laboratory, LA7997-MS.

18. Naber, J. D. and Reitz, R. D., "Modeling engine spray/wall impingement", SAE Paper NO. 880107; 1988.

19. Halstead, M., Kirsch, L. and Quinn, C., "The Auto ignition of hydrocarbon fueled at high temperatures and pressures - fitting of a mathematical model", *Combustion Flame,* Vol. 30, (1977), 45-60.

20. Patterson, M. A., Kong, S. C., Hampson, G. J. and Reitz, R. D., "Modeling the effects of fuel injection characteristics on diesel engine soot and NOx emissions", SAE Paper NO. 940523; 1994.

21. Khoushbakhti Saray, R., Mohammahi Kusha, A. and Pirozpanah, V., "A new strategy for reduction of emissions and enhancement of performance characteristics of dual fuel engine at part loads", *International Journal of Engineering*, Vol. 23, (2010), 87-104.

22. Heywood, J. B., "Internal combustion engine fundamental", New York: McGraw Hill Book Company; 1988, 568-586.

23. Sbastian, S. and Wolfgang, S., "Combustion in a swirl chamber diesel engine simulation by computation of fluid dynamics", SAE Paper NO. 950280; 1995.

24. Yoshihiro, H., Kiyomi, N. and Minaji, I., "Combustion improvement for reducing exhaust emissions in IDI diesel engine", SAE Paper NO. 980503; 1998.

25. Hajireza, S., Regner, G., Christie, A., Egert, M. and Mittermaier, H., "Application of CFD modeling in combustion bowl assessment of diesel engines using DoE methodology", SAE Paper NO. 2006-01-3330; 2006.

26. Carsten, B., "Mixture formation in internal combustion engines", Berlin: Springer publications; 2006, 226-231.

Multi-Dimensional Modeling of the Effects of Spilt Injection Scheme on Performance and Emissions of IDI Diesel Engines

S. Jafarmadar, A. Zehni

Department of mechanical Engineering, University of Urmia, Urmia, Iran

---

چکیده

یکی از مسائل مهم در کاهش آلایندگی موتورهای دیزلی تزریق مستقیم و غیر مستقیم مصالحه بین آلایندههای اکسید نیتروژن و دوده میباشد. تزریق چند گانه یکی از مهمترین روشهای کاهش این مصالحه میباشد. در کار حاضر، تأثیر تزریق چند گانه بر فرآیندهای احتراق و آلایندگی یک موتور دیزلی تزریق غیر مستقیم تحت شرایط توان بیشینه ۵/۹ کیلووات و ۷۳۰ دور بر دقیقه بررسی شده است. پارامترهای زمان تزریق، فاصله پاشش بین پالسهای تزریق و مقدار سوخت پاششی بررسی شدهاند. همچنین سه حالت مختلف تزریق چند گانه که در آنها به ترتیب ۱۰، ۲۰ و ۲۵ درصد کل سوخت پاششی در پالس دوم میباشد مطالعه شده است. نتایج عددی نشان میدهند که حالت بهینه پاشش به صورت ۲۵ درصد کل سوخت پاششی در پالس دوم تزریق به همراه ۲۰ درجه میللنگ فاصله بین پالسهای اول و دوم پاشش میباشد. نتایج عددی احتراق و آلایندگی بهدست آمده توافق خوبی با نتایج تجربی دارد که میتواند چشمانداز مناسبی برای مفاهیم جدید علم موتور باشد

doi: *10.5829/idosi.ije.2012.25.02c.07*